

On the Properties of the Cr_{1+x}Sb , Fe_{1+x}Sb , Co_{1+x}Sb , Ni_{1+x}Sb , Pd_{1+x}Sb , and Pt_{1+x}Sb Phases

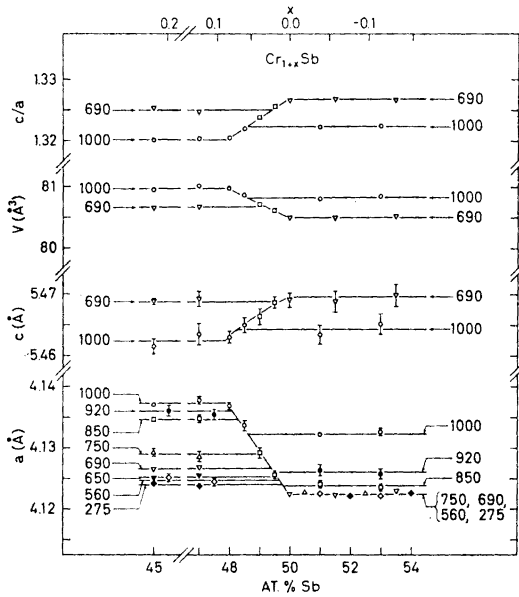
ARNE KJEKSHUS and KJELL P. WALSETH

Kjemisk Institutt A, Universitetet i Oslo, Blindern, Oslo 3, Norway

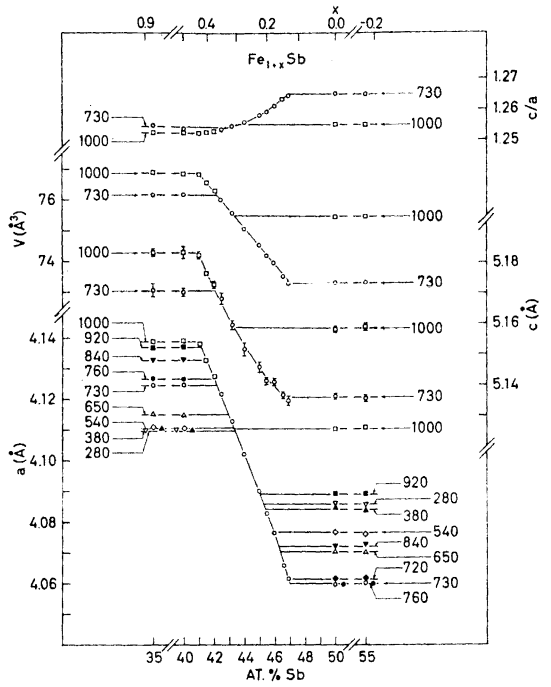
The mono-antimonide phases of chromium, iron, cobalt, nickel, palladium, and platinum have been studied by means of X-ray diffraction, density, and metallographic measurements. The results show that these phases can be characterized by the general formula $T_{1+x}\text{Sb}$ where T denotes the metal component and x may be positive, negative, or zero. The extensions of the homogeneity ranges are appreciably temperature dependent for all phases, but only for Co_{1+x}Sb and Ni_{1+x}Sb do these regions extend on both sides of 50 atomic %. The basic, NiAs type crystal structure has been confirmed for all phases, and the additional (for $x > 0$) and subtractional (for $x < 0$) natures of the solid solutions have been verified.

Phases with the NiAs type crystal structure are commonly found in the equiatomic regions of the transition metal systems with the pnigogen and chalcogen elements (*cf.* Ref. 1). Although these phases often exhibit broad ranges of homogeneity, their composition regions seldom include the equiatomic ratio. The nickel mono-antimonide phase appears to be hitherto the only definite example of a phase with this structure type, whose composition range extends on both sides of 50 atomic %.^{2,3} The available data^{3,4} suggest furthermore that the cobalt mono-antimonide phase provides another example of this behaviour. In fact, the antimonides form an interesting sub-class of the phases with this structure type since the transition metal component can be varied both horizontally (Ti to Ni) and vertically (Ni to Pt) in the Periodic System. (The symbol T is used throughout this paper as a common abbreviation for the elements (Ti, V,) Cr, (Mn,) Fe, Co, Ni, Pd, and Pt.)

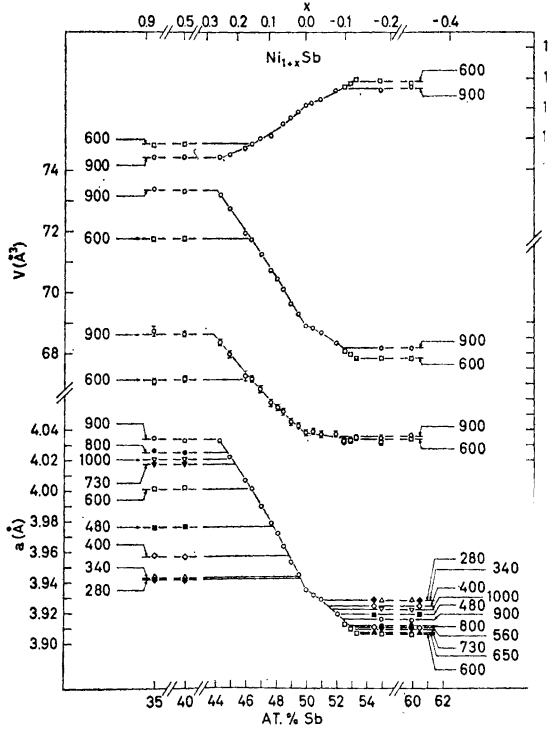
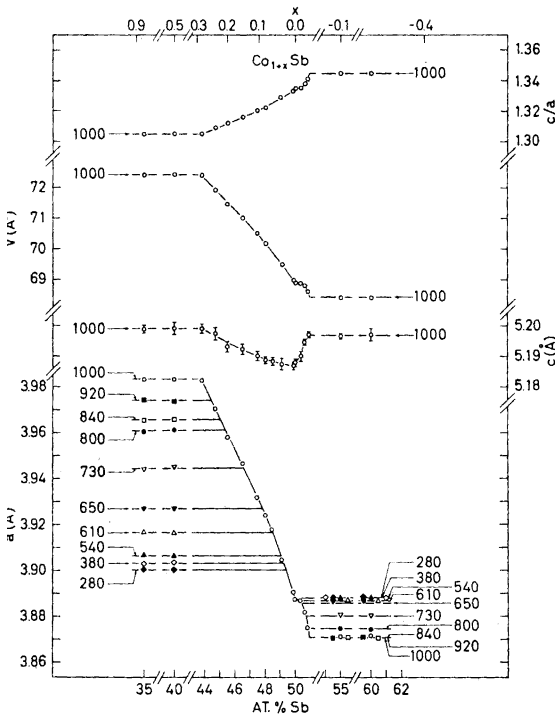
With the exception of the systems Ti-Sb and V-Sb, which have been studied only since 1950, the first investigations of the other T -Sb systems were made at the beginning of this century by thermal analysis and microscopy. However, despite numerous studies of the Ti_{1+x}Sb ,⁵⁻⁹ V_{1+x}Sb ,^{6,10-12} Cr_{1+x}Sb ,^{8,13-29} Mn_{1+x}Sb ,^{8,13-15,18,20-22,24,26,28-37} Fe_{1+x}Sb ,^{3,8,14,15,35,38-44} Co_{1+x}Sb ,^{3,4,8,14,15,23,28,35,43-48} Ni_{1+x}Sb ,^{2,3,8,14,15,35,43,44,47-53} Pd_{1+x}Sb ,⁵⁴⁻⁵⁹ and Pt_{1+x}Sb ,^{58,60-64} phases the knowledge of the extensions of the homogeneity ranges is incomplete and often controversial, and their temperature depend-



(a)



(b)



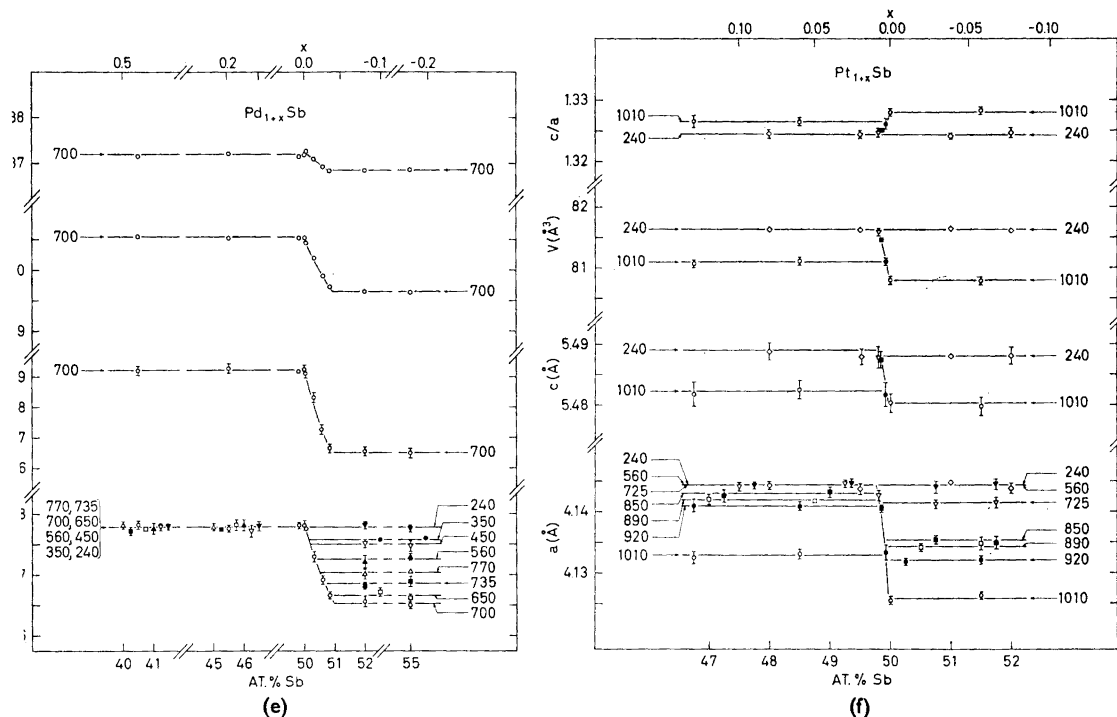


Fig. 1. Unit cell dimensions versus composition for (a) Cr_{1+x}Sb , (b) Fe_{1+x}Sb , (c) Co_{1+x}Sb , (d) Ni_{1+x}Sb , (e) Pd_{1+x}Sb , and (f) Pt_{1+x}Sb . The vertical bars represent the uncertainty when the calculated error limit exceeds the size of the symbols. The numbers indicated on the diagrams give the annealing temperatures in $^{\circ}\text{C}$.

ences are virtually unknown. The main purpose of the present investigation has been to provide such information. Ti_{1+x}Sb , V_{1+x}Sb , and Mn_{1+x}Sb have not been studied in any detail since these phases have recently been subjected to examination^{9,12,37} at this Institute, but some of our preliminary data for the Mn_{1+x}Sb phase are included for the sake of completeness.

It is hoped that the acquisition of additional information will help to reduce the amount of pure speculation which has prevailed in the literature in connection with phases having the NiAs type structure.

EXPERIMENTAL

The pure elements used in this study were 99.999% Cr (Koch-Light Laboratories, Ltd.), 99.99+ % Fe, 99.999% Co, and 99.995% Ni (Johnson, Matthey & Co., Ltd.; turnings from rods), 99.99% Pd (L. Light & Co., Ltd.), and 99.999% Pt and Sb (Johnson, Matthey & Co., Ltd.). The samples were prepared by heating weighed quantities of the components in evacuated and sealed silica tubes at temperatures between 850 and 1250 $^{\circ}\text{C}$ for about 20 h. The sintered powders were ground and reannealed over periods ranging from 3 days to 2 months at fixed temperatures between 240 and 1010 $^{\circ}\text{C}$ and finally

quenched in ice water without shattering the enclosing silica capsules. One series of samples from each system was also cooled slowly from 500°C to room temperature over a period of 2 months.

X-Ray powder photographs of all samples were taken in a Guinier type camera of 80 mm diameter with monochromatized $\text{CuK}\alpha_1$ -radiation ($\lambda=1.54050 \text{ \AA}$) using KCl as internal standard. The lattice dimensions were refined by applying the method of least squares to the diffraction data and the indicated error limits correspond to twice the standard deviations obtained in these calculations. The integrated intensities of the reflections were measured photometrically. Atomic scattering factors were taken from *International Tables*.⁶⁵

The density measurements were made pycnometrically at 25.00°C with kerosene as displacement liquid. To remove gases adsorbed by the sample (weighing $\sim 2 \text{ g}$), the pycnometer was filled with kerosene under vacuum.

Metallographic specimens were prepared using araldite as mounting material. After grinding and mechanical polishing (first with a fine grained diamond paste and finally with levigated alumina), the specimens were etched, in most cases in aqueous solutions of HNO_3 or $\text{HNO}_3 + \text{FeCl}_3$. The microindentation hardness measurements were performed with a Reichert microhardness tester (No. 1109) used in combination with a Reichert universal camera microscope (model MeF). Two different loads (42 and 84 g) were used on the indenter, which was a Vickers pyramid. Several readings (at each load) were taken across a given section of the specimen and measurements were repeated at different grinding depths.

RESULTS

(i) *Variations of the unit cell dimensions with composition.* The unit cell dimensions of the various $T_{1+x}\text{Sb}$ phases as functions of compositions are shown in Fig. 1a-f. A common feature of the diagrams is that the a -axis decreases with increasing content of Sb, whereas the individual composition dependences of the c -axes for the Cr_{1+x}Sb and Co_{1+x}Sb phases destroy the general pattern for the latter parameter. The lattice dimensions vary continuously with the composition throughout the homogeneity ranges of all phases. For the Co_{1+x}Sb and Ni_{1+x}Sb phases, whose homogeneity ranges extend on both sides of 50 atomic %, discontinuous changes in the slopes of the a , c , V , and c/a versus composition (in atomic % Sb) curves are found at the equi-atomic composition. The latter findings are in accordance with expectation since a notable structural difference is associated with the change from $x < 0$ to $x > 0$ in the formula $T_{1+x}\text{Sb}$ (see section iv).

(ii) *Homogeneity ranges.* The extensions of the homogeneity ranges and their temperature variations have been determined from the unit cell dimensions of quenched samples (*cf.* Fig. 1a-f). An inevitable uncertainty connected with the results obtained by this method is that it is difficult to obtain quenching rates high enough to ascertain that quenched samples really reflect the true thermodynamic equilibrium at the annealing temperature. Considerable attention was therefore paid to this problem by the choice of thin-walled quartz tubes for the capsules, *etc.*, and the internal consistency of the various sets of data may indicate that the attempts have been successful. The phase limits (in particular those at the highest temperatures) presented here should nevertheless be considered as minimum values for the extensions of the homogeneity ranges.

The composition dependence of the a -axes is used for evaluation of the phase limits in preference to the corresponding c -axis relationships, since the former parameter generally shows the larger relative variation of the two

and furthermore carries the narrowest error limits. The method used in these determinations is clearly illustrated in Fig. 1a—f, where the region of homogeneity at a given temperature is defined by that part of the inclined line lying between points of intersection with the horizontal lines corresponding to the temperature concerned. The extensions of the homogeneity regions so defined have been verified by using the same process in respect of the parameters c , V , and c/a . The accuracy, which clearly depends on the angles of intersection, is somewhat less in the latter cases. The overall upper and lower limits of the homogeneity ranges were confirmed using the disappearing phase principle on the Guinier photographic data.

The derived dependences of the various homogeneity ranges on temperature are shown in Fig. 2 in relation to the relevant parts of the liquidus curves

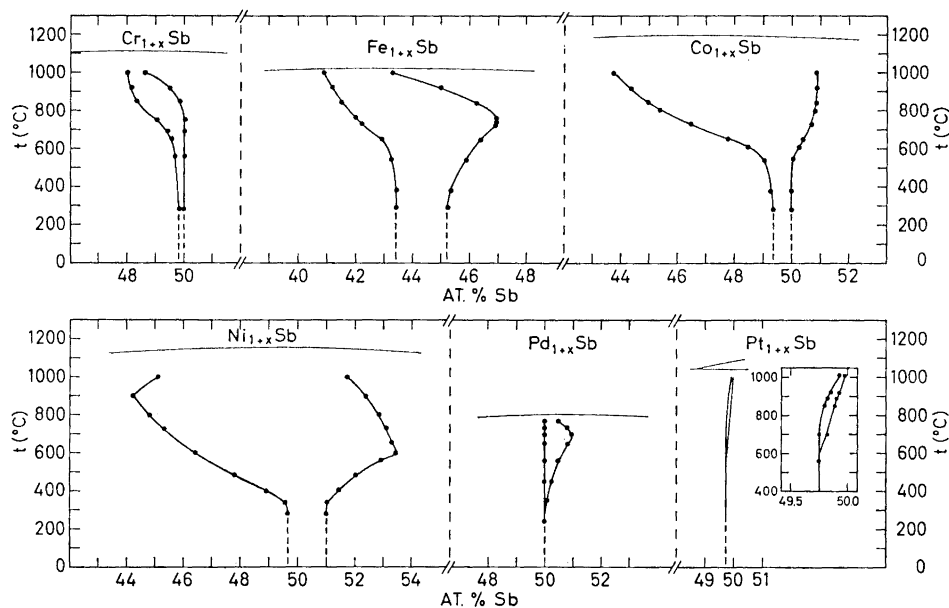


Fig. 2. Extensions of the homogeneity ranges for the $T_{1+x}\text{Sb}$ phases as functions of temperature.

taken from the compilation by Hansen.^{66,67} The probable form of the characteristics at the lowest temperatures is indicated in the diagrams by broken lines. (The slowly cooled samples gave identical results with those quenched from 240–280°C). The present findings differ appreciably from the data presented by Hansen where the homogeneity ranges are represented as being less dependent on temperature. The form of the characteristics (Fig. 2) shows a substantial variation between the phases, a progressive broadening being notable in the T -sequence Cr-Fe-Co-Ni while a rapid narrowing occurs within the sequence Ni-Pd-Pt. There is also a degree of correlation of the maximum extension of the homogeneity ranges with such factors as the radius

ratio r_T/r_{Sb} and the electronegativity difference between Sb and T . $Fe_{1+x}Sb$ differs appreciably from the other phases in that its homogeneity range is nowhere nearer the equiatomic composition than 3 atomic %.

(iii) *Verification of the formula $T_{1+x}Sb$.* On comparison of the pycnometric densities with those calculated from the X-ray data (Fig. 3) it is clear that

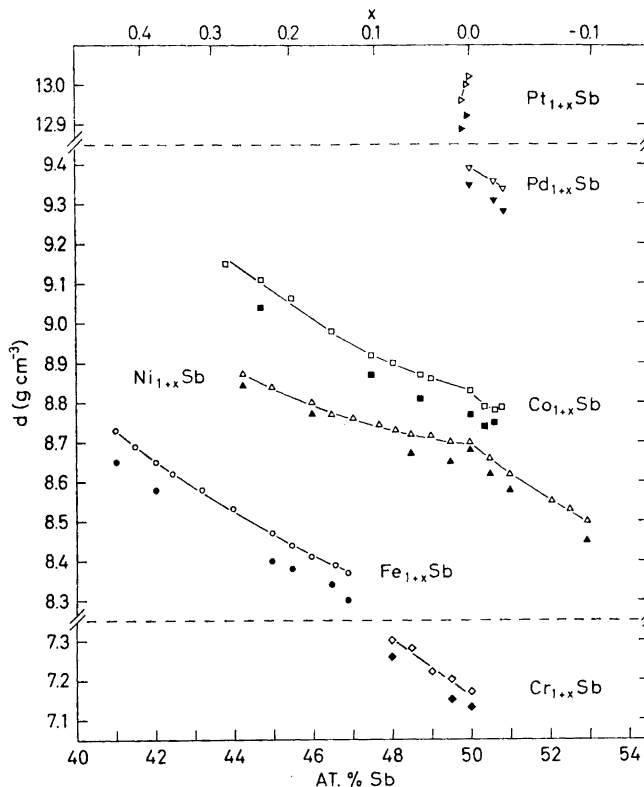


Fig. 3. Observed (open symbols) densities of the $T_{1+x}Sb$ phases as a function of composition and those calculated (corresponding filled symbols) from the X-ray data on the basis of additional ($x > 0$) or subtractional ($x < 0$) solid solutions (see text).

T atoms are added to the ideal NiAs lattice for compositions < 50 atomic % Sb and are subtracted when the Sb content is > 50 atomic %. This justifies the use of the general formula $T_{1+x}Sb$. A possible exception occurs in the case of $Pt_{1+x}Sb$ where the narrowness of the homogeneity range and its proximity to the equiatomic composition prevent definite conclusions from being drawn.

(iv) *Atomic arrangement.* It is well known (*cf.* Ref. 1) that the NiAs type structure occupies a position which is intermediate between those of Ni_2In and $Cd(OH)_2$. The transition between the structure types is achieved by an occupation of the trigonal bipyramidal holes by metal atoms on going

from that of NiAs to Ni₂In on one hand and a removal of alternate layers of metal atoms, on going from NiAs to Cd(OH)₂. The crystallographic description of the atomic arrangement in the ideal NiAs type structure is as follows, in terms of the space group $P6_3/mmc$: $2T_{\text{I}}$ in (a) 0,0,0; 0,0,1/2 and 2Sb in (c) 1/3,2/3,1/4; 2/3,1/3,3/4. The additional T atoms incorporated in the lattice when $x > 0$ occupy the position (d) of the same space group at random, *i.e.* $2xT_{\text{II}}$ in (d) 1/3,2/3,3/4; 2/3,1/3,1/4. For $x < 0$, the vacant lattice sites are conveniently considered to be randomly distributed on, say, 0,0,1/2, implying a necessary change of the space group (to $P\bar{3}m1$).

Comparison of observed and calculated X-ray intensities confirms that the basic structure is of the NiAs type for these T_{1+x} Sb phases. In those cases where the departure from stoichiometry is particularly large, *i.e.* for $x > \sim 0.2$ in the Fe_{1+x}Sb, Co_{1+x}Sb, and Ni_{1+x}Sb phases, unambiguous confirmation of the nature of the defect (Ni₂In/NiAs type) structure has also been possible.

The NiAs type structure can exist with interstitial atoms as well as vacant sites in the lattice, both kinds of defects occur, for example, within the homogeneity ranges of the Co_{1+x}Sb and Ni_{1+x}Sb phases. The supposition of a degree of disorder between the T_{I} and T_{II} sites may accordingly be considered as eminently possible (even at the stoichiometric 1:1 composition). However, within the limitation set by the accuracy of the present measurements of X-ray intensities no indication of the occurrence of such disorder could be detected. In terms of percentage, this type of disorder corresponds to less than $\sim 5\%$ transfer of T atoms between the T_{I} and T_{II} sub-lattices (thus creating vacancies in the T_{I} sub-lattice; *vide supra*).

In the NiAs type structure (at the stoichiometric 1:1 composition and with perfect lattice order) each metal atom is octahedrally coordinated to six near non-metal atoms and each non-metal atom is surrounded by six near metal atoms in a trigonal prismatic configuration. However, both types of coordination polyhedra are somewhat deformed in the present T_{1+x} Sb phases as clearly evidenced by their octahedral (80.84–83.75° and the corresponding supplements) and trigonal prismatic (99.16–96.25, 56.94–61.40, and 127.84–129.07°) angles. In the ideal NiAs type structure, where $c/a = \sqrt{8/3} = 1.633\dots$, the octahedral angles are 90° and the relevant trigonal prismatic angles 90, 70.54, and 130.81°.

The composition dependences of the shortest interatomic distances are shown in Fig. 4. It is seen that the $T_{\text{I}}\text{—Sb}$ and $T_{\text{II}}\text{—Sb}$ distances decrease almost linearly with increasing composition in atomic % Sb, and that especially for the phases Cr_{1+x}Sb, Fe_{1+x}Sb, Co_{1+x}Sb, and Ni_{1+x}Sb, have virtually parallel dependences. The shift of level of 0.3–0.4 Å between the $T_{\text{I}}\text{—Sb}$ and $T_{\text{II}}\text{—Sb}$ separations, suggests that the bonding to Sb of these crystallographically non-equivalent T atoms is of a different character in the two cases. The values of the shortest $T_{\text{I}}\text{—}T_{\text{I}}$ and $T_{\text{I}}\text{—}T_{\text{II}}$ (equal to the $T_{\text{I}}\text{—Sb}$ distances shown on the diagram for $x > 0$) separations are consistent with a strong bonding interaction between these atoms.

(v) *Microhardness.* The composition dependences of microindentation hardness shown in Fig. 5 exhibit a general decrease with increasing Sb content. This kind of characteristic is in accordance with a weakening of the lattice

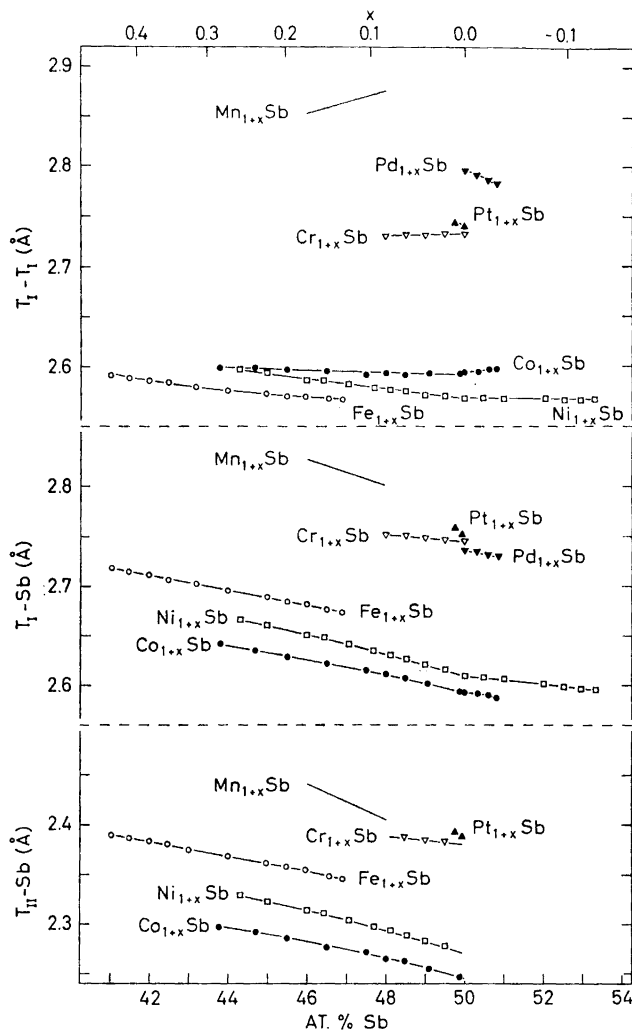


Fig. 4. The shortest interatomic distances in the $T_{1+x}Sb$ phases as a function of composition.

with progressive removal of T atoms and the consequent decrease in the total number of bonds, provided, of course, that changes due to such factors as dislocation density are negligible.

The inset diagram shows a normal increase of melting point with microhardness at the equiatomic composition (extrapolated to 50 atomic % for the $Fe_{1+x}Sb$ phase).

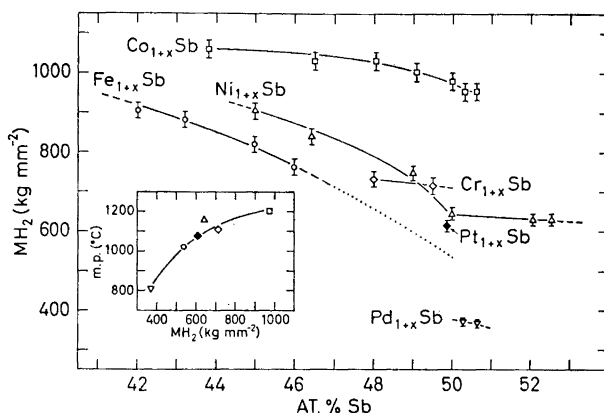


Fig. 5. Microindentation hardness (at constant load = 84 g) of the $T_{1+x}Sb$ phases as a function of composition. The vertical bars indicate the inaccuracies. The inset shows melting point (taken from Hansen ^{66,67}) versus microindentation hardness at 50 atomic %.

REFERENCES

1. Kjekshus, A. and Pearson, W. B. *Progr. Solid State Chem.* **1** (1964) 83.
2. Shibata, N. *Sci. Rep. Tohoku Univ., First Ser.* **29** (1941) 697.
3. Ageev, N. V. and Makarov, E. S. *Izv. Akad. Nauk SSSR Otd. Khim. Nauk* **1943** 87.
4. Dudkin, L. D. and Abrikosov, N. Kh. *Zh. Neorg. Khim.* **1** (1956) 2096.
5. Nowotny, H. and Pesl, J. *Monatsh.* **82** (1951) 336.
6. Nowotny, H., Funk, H. and Pesl, J. *Monatsh.* **82** (1951) 513.
7. Shchukarev, S. A., Morozova, M. P. and Li, M. S. *J. Gen. Chem. SSSR (English Transl.)* **29** (1959) 2427.
8. Adachi, K. *J. Phys. Soc. Japan* **16** (1961) 2187.
9. Kjekshus, A., Grønvald, F. and Thorbjørnsen, J. *Acta Chem. Scand.* **16** (1962) 1493.
10. Grison, B. and Beck, P. A. *Acta Cryst.* **15** (1962) 807.
11. Meissner, H. G. and Schubert, K. *Z. Metallk.* **56** (1965) 523.
12. Leonardsen, E. and Røst, E. *To be published.*
13. Williams, R. S. *Z. anorg. Chem.* **55** (1907) 7.
14. Oftedal, I. *Z. physik. Chem.* **128** (1927) 135.
15. de Jong, W. F. and Willems, H. M. V. *Physica* **7** (1927) 74.
16. Masing, G. and Wallbaum, H. J. *Nachr. Akad. Wiss. Göttingen, Math.-Phys. Kl.* **1941** 32.
17. Haraldsen, H., Rosenqvist, T. and Grønvald, F. *Arch. Math. Naturv.* **1948** No. 4.
18. Guillaud, C. *Ann. Phys.* **4** (1949) 671.
19. Snow, A. I. *Phys. Rev.* **85** (1953) 365.
20. Matthias, B. T. *Phys. Rev.* **92** (1953) 365.
21. Hirone, T., Maeda, S., Tsubokawa, J. and Tsuya, N. *J. Phys. Soc. Japan* **11** (1956) 1083.
22. Lotgering, F. K. and Gorter, E. W. *J. Phys. Chem. Solids* **3** (1957) 238.
23. Abrikosov, N. Kh. *Izv. Akad. Nauk SSSR, Ser. Fiz.* **21** (1957) 141.
24. Suzuoka, T. *J. Phys. Soc. Japan* **12** (1957) 1344.
25. Fakidov, I. G. and Afanas'ev, A. Ya. *Fiz. Metal. Metalloved.* **6** (1958) 176.
26. Tsubokawa, I. *J. Phys. Soc. Japan* **16** (1961) 277.
27. Wendling, R. *Compt. Rend.* **252** (1961) 3423.
28. Suchet, J. J. *Phys. Radium* **23** (1962) 497.
29. Takei, W. J., Cox, D. E. and Shirane, G. *Phys. Rev.* **129** (1963) 2008.
30. Halla, F. and Nowotny, H. *Z. physik. Chem.* **B 34** (1936) 141.

31. Pfisterer, H. and Schubert, K. *Z. Metallk.* **41** (1950) 358.
32. Willis, B. T. M. and Rooksby, H. P. *Proc. Roy. Soc. (London)* **B 67** (1954) 290.
33. Fischer, G. and Pearson, W. B. *Can. J. Phys.* **36** (1958) 1010.
34. Piekart, S. J. and Nathans, R. *J. Appl. Phys.* **30** (1959) 280S.
35. Schmid, H. *Cobalt* **7** (1960) 26.
36. Schukarev, N. S., Morozova, N. S. and Stolyarova, T. A. *J. Gen. Chem. SSSR (English Transl.)* **31** (1961) 1657.
37. Grønvold, F. and Snildal, S. *To be published.*
38. Kurnakov, N. S. and Konstantinov, N. S. *Z. anorg. Chem.* **58** (1908) 1.
39. Hägg, G. *Z. Krist.* **A 68** (1928) 470.
40. Hägg, G. *Nova Acta Reg. Soc. Sci. Upsaliensis Ser. 4* **7** (1929) No. 1.
41. Oftedal, I. *Z. physik. Chem.* **B 4** (1929) 67.
42. Fournier, P. *Rev. Chim. Ind.* **44** (1935) 195.
43. Alekseevskii, N. *Zh. Eksp. Teor. Fiz.* **18** (1948) 101.
44. Geiderikh, V. A. and Gerasimov, Ya. I. *Russ. J. Phys. Chem.* **37** (1963) 1274.
45. Kurnakov, N. S. and Podkopajev, L. *Zh. Russ. Fiz.-Khim. Obschestva* **38** (1906) 463.
46. Lewkonja, K. *Z. anorg. Chem.* **59** (1908) 293.
47. Fürst, U. and Halla, F. *Z. physik. Chem.* **B 40** (1938) 285.
48. Rosenqvist, T. *Acta Met.* **1** (1953) 761.
49. Lossev, K. *Z. anorg. Chem.* **49** (1906) 58.
50. de Jong, W. F. *Physica* **5** (1925) 241.
51. Schneider, A. and Imhagen, K. H. *Naturwiss.* **44** (1957) 324.
52. Matthias, B. T., Geballe, T. H. and Compton, V. B. *Rev. Mod. Phys.* **35** (1963) 1.
53. Wägini, H. *Z. Naturforsch.* **21a** (1966) 362.
54. Sander, W. *Z. anorg. Chem.* **75** (1912) 97.
55. Thomassen, L. *Z. physik. Chem.* **135** (1928) 383.
56. Grigorjev, A. T. *Z. anorg. allgem. Chem.* **209** (1932) 308.
57. Schubert, K. and Beskow, H. *Naturwiss.* **40** (1953) 269.
58. Matthias, B. T. *Phys. Rev.* **90** (1953) 487.
59. Jan, J.-P., Pearson, W. B. and Springford, M. *Can. J. Phys.* **42** (1962) 2357.
60. Friedrich, K. and Leroux, A. *Metallurgie* **6** (1909) 1.
61. Guertler, W. *Metallographic*, Borntraeger, Berlin 1912, Vol. I, p. 773.
62. Thomassen, L. *Z. physik. Chem.* **B 2** (1929) 349.
63. Thomassen, L. *Z. physik. Chem.* **B 4** (1929) 277.
64. Nemilov, W. A. and Waronov, N. V. *Z. anorg. allgem. Chem.* **226** (1936) 177.
65. *International Tables for X-Ray Crystallography*, Kynoch Press, Birmingham 1962, Vol. III.
66. Hansen, M. (and Anderko, K.) *Constitution of Binary Alloys*, McGraw, New York-Toronto-London 1958.
67. Hansen, M. (Revised edition by Elliott, R. P.) *Constitution of Binary Alloys, First Supplement*, McGraw, New York-St. Louis-San Francisco-Toronto-London-Sydney 1965.

Received February 10, 1969.